RSC Advances

PAPER

View Article Online
View Journal | View Issue

Cite this: *RSC Adv.*, 2015, **5**, 54090

Unsaturated aldehydes: a novel route for the synthesis of pyridine and 3-picoline

Cai-Wu Luo and Zi-Sheng Chao*

Received 26th December 2014
Accepted 23rd February 2015

DOI: 10.1039/c4ra17098a

www.rsc.org/advances

A novel reaction pathway was developed for the synthesis of pyridine and 3-picoline from the condensation of gas-phase acrolein dimethyl acetal or acrolein diethyl acetal and ammonia over various catalysts in a fixed-bed reactor. ZnO loaded on alkaline–acid sequentially-treated HZSM-5, namely ZnO/HZSM-5-At-acid, was prepared and employed in these reactions for the first time. 3-Picoline, without the generation of 4-picoline, was obtained from the condensation of acrolein dimethyl acetal and ammonia. The ZnO/HZSM-5-At-acid catalyst was proven to be the most promising catalyst relative to other catalysts in this study. The stability of the ZnO/HZSM-5-At-acid catalyst was remarkably higher than that of the ZnO/HZSM-5 catalyst. The catalysts were characterized using XRD, ^{27}Al MAS NMR, XPS, UV-vis DRS, N_2-physisorption, NH_3-TPD and TG technologies and the results revealed that the pore structure, acidity and location of ZnO had great influence on the total yield of pyridine and 3-picoline, and the catalyst stability.

1. Introduction

3-Picoline, as a key chemical intermediate, is widely used as a building block for the synthesis of pesticides, fodder and pharmaceuticals.[1] The industrial synthesis of 3-picoline is conducted with formaldehyde, acetaldehyde and ammonia over HZSM-5 containing catalysts.[2] In this route, the yield of 3-picoline is no more than 27% and a lot of pyridine is generated. As a better alternative, a higher yield of 3-picoline is obtained from the condensation of acrolein and ammonia. For example, some patents report that the condensation of acrolein and ammonia can be conducted,[3] to which a third component such as acetaldehyde[4] or propionaldehyde[5] can be added, and 30–60% yield of 3-picoline is obtained. However, the biggest problem of these routes is that the reactions have to stop after a short time due to the blocking of the reactor from polymerization. Additionally, the reactants possess chemical instability and extreme toxicity, which makes it hard to meet increasing environmental requirements. It is noted that the lifetime of the catalyst has still been a great challenge in all the gas-phase synthesis methods up to now.

In the present work, we report a novel route for the synthesis of pyridine and 3-picoline from the condensation of gas-phase acrolein dimethyl acetal or acetal diethyl acetal and ammonia over various catalysts in a fixed-bed reactor. These acetals easily decompose into acrolein and methanol or ethanol in the presence of an acid catalyst. In this case, the problem of polymerization is consequently solved. 3-Picoline, without the generation of 4-picoline, is obtained in the condensation of gas-phase acrolein dimethyl acetal and ammonia. Using acrolein diethyl acetal as the starting material can transform biological resources instead of traditional resources into pyridine and 3-picoline, because acrolein is easily produced in the dehydration of bio-glycerol. This enlarges the scope of the synthesis of pyridine and 3-picoline, and meanwhile, it also provides a very useful reference for solving the problem of polymerization from acrolein or unsaturated aldehydes (or ketones). The novelty of this work is that it also reports that MgF_2/HZSM-5 and ZnO/HZSM-5-At-acid catalysts are prepared and these novel catalysts are employed in the synthesis of pyridine and 3-picoline. Satisfactory yields of pyridine and 3-picoline are obtained and a longer stability for the ZnO/HZSM-5-At-acid catalyst is also obtained.

2. Experimental

2.1. Chemical

All the chemicals of analytic purity, such as acrolein dimethyl acetal, were purchased commercially.

Various zeolites, such as HZSM-5 and HY catalysts, were supplied by Nankai University. Thes catalysts were calcined at 550 °C for 4 h before use.

2.2. Catalyst preparation

The MgF_2/HZSM-5 catalyst was synthesized using a two-step sequential-treatment method. In brief, 32.5 g HZSM-5 was added into a solution containing 0.155 M $Mg(NO_3)_2$ in 100 mL H_2O and 1.0 mL concentrated HNO_3, and they were treated at 100 °C for 8 h under vigorous stirring and reflux conditions. Then, the mixture was dried at 120 °C for 12 h. The dried

College of Chemistry and Chemical Engineering, State Key Laboratory of Chem/Biosensing and Chemometrics, Hunan University, Changsha 410082, China. E-mail: zschao@hnu.edu.cn; zschao@yahoo.com; Tel: +86-731-88713257

material was stirred with a solution containing 0.155 M NH_4F and HF (molar ratio of $NH_4F/HF = 1/1$) in 100 mL H_2O, and they were treated at 100 °C for 12 h under vigorous stirring and reflux conditions. Then, the mixture was dried at 120 °C for 12 h. Finally, it was calcined at 700 °C for 4 h. The resulting catalyst was denoted as MgF_2/HZSM-5. A similar method is used for the preparation of the MgF_2/Al_2O_3 catalysts (different types of Al_2O_3).

HZSM-5 was further modified with $Zn(NO_3)_2$, H_2SO_4 and KF solutions using the wet-impregnation method, and ZnO/HZSM-5, H_2SO_4/HZSM-5 and KF/HZSM-5 were obtained, respectively. The content of the active components (Zn, H_2SO_4 and KF) was fixed at 1 wt%. The Zn–M (M: Fe, Co, Ni, Mo)/HZSM-5 catalysts were prepared by the impregnation of ZnO/HZSM-5 with metal (M) nitrate containing solutions at room temperature for 24 h under vigorous stirring, followed by drying overnight and calcination at 500 °C for 4 h in air. The content of M was fixed at 0.5 wt%.

The HZSM-5-At and HZSM-5-At-acid catalysts were synthesized using a similar method to that reported in ref. 6. In brief, 100 mL of 0.20 M NaOH solution was first added into a 500 mL three-neck flask and was heated to 80 °C under vigorous stirring, and then 10 g of HZSM-5 was quickly added to the above solution. The resulting suspension was stirred for 0.5 h. After cooling, the solid was repeatedly washed with deionized water until the pH became neutral, and was dried at 120 °C for 12 h. The dried catalyst was ion-exchanged with 1.0 M NH_4Cl solution (80 °C, 4 h), followed by filtration and washing with deionized water. The above process was repeated three times. Finally, the product was calcined at 550 °C for 4 h. The resulting catalyst was denoted as HZSM-5-At. The prepared catalyst was further acid-treated with 0.1 M HCl at 70 °C for 6 h. After this treatment, the catalyst was filtered, washed, dried and calcined at 550 °C for 4 h. The resulting catalyst was denoted as HZSM-5-At-acid.

The ZnO/HZSM-5-At-acid catalyst was prepared by impregnation of HZSM-5-At-acid with Zn $(NO_3)_2$ solution at room temperature for 24 h under vigorous stirring, followed by drying overnight and calcination at 500 °C for 4 h in air. The content of Zn was fixed at 1 wt%.

All the catalysts investigated in the present work were pressed, crushed, and sieved to 20–40 mesh before use.

2.3. Characterization

X-ray diffraction spectroscopy (XRD) was performed with Bruker D8-Advance X-ray diffraction equipment, under the following conditions: Cu target K_α ray ($\lambda = 1.54187$ Å), scanning voltage 40 kV, scanning current 40 mA, scanning speed 0.5 s and scanning step 0.02°.

The ^{27}Al magic angle spinning (MAS) NMR spectrum was recorded at a spinning speed of 12 kHz on a Bruker Avance III 400 MHz standard-bore spectrometer equipped with a 4 mm probe head.

X-ray photoelectron spectroscopy (XPS) experiments were carried out using a PHI Quantum 2000 instrument with a Al K_α radiation source. A suitable amount catalyst was compressed into a wafer for analysis. The signal of carbon C 1s was present at 284.6 eV.

Diffuse reflectance ultraviolet-visible spectroscopy (UV-vis DRS) was carried out on a Lambda 35 equipped with an integration sphere (Perkin Elmer Corp.). The wavelength was detected at 200–800 nm.

N_2 adsorption–desorption measurements were carried out at liquid nitrogen temperature using a Quantachrome instrument. The catalyst was loaded in this apparatus for outgassing at 300 °C until a vacuum of 10^{-8} Torr was attained and was kept under this vacuum for an additional 12 h. The specific surface area was determined using the BET method and the pore volume was calculated at a relative pressure of $p/p_0 \approx 0.99$, assuming full surface coverage with nitrogen.

Ammonia temperature-programmed desorption (NH_3-TPD) experiments were carried out using an Autochem II 2920 instrument. The catalyst was dried in flowing helium (99.99%, 60 mL min^{-1}) at 400 °C for 0.5 h prior to NH_3 adsorption. NH_3 adsorption took place at 100 °C until saturation, and then the catalyst was flushed with helium at the same temperature for 1 h. TPD measurements were conducted from 100 °C to 800 °C, with a heating rate of 10 °C min^{-1}.

Thermogravimetry (TG) profiles were recorded on a Diamond instrument (Perkin Elmer Corp.). The catalyst was heated from room temperature to 800 °C in an air stream at a heating rate of 5 °C min^{-1}. The flow rate of air was 30 mL min^{-1}. In the recorded profiles, the weight loss before 300 °C was attributed to the desorption of water. The decrease in weight from 300 °C to 800 °C was caused by burning off the coke.

2.4. Catalytic performance evaluation

The gas-phase condensation of reagents was conducted under atmospheric pressure in a vertical fixed-bed stainless steel reactor (i.d. 10 mm). Unless otherwise specifically mentioned, the reactor was packed as follows: the middle of the reactor was plugged with the support, and the catalyst (about 1.50 g) was located over it. The reactor was placed into a tubular furnace with the catalyst bed located in the constant temperature zone. A thermocouple was employed to monitor and control the temperature. Prior to the reaction, the reactor was pretreated at 500 °C in a flow of air, and was then cooled to a suitable temperature. After switching the air to nitrogen, the reaction was started. The reaction feeds (containing acetals, water, ammonia and nitrogen) were preheated at 250 °C, and then they were fed into the reactor. The reaction products were diluted with alcohol, condensed in an ice-water trap and collected for analysis on a GC equipped with an ATTM-AQUAWAX-DA capillary column (i.d. 60 m × 0.25 μm × 0.32 mm) and a FID detector. The reaction continued for 3 h and the liquid products were abandoned at TOS = 0–1 h due to the induction period of the catalysts. A suitable amount of internal standard (1-butanol) was added to the liquid products prior to analysis for quantitative determination. The acetal was completely converted under all the reaction conditions. The yields of pyridine and 3-picoline were calculated according to the following equation:

$$\text{Yield (mol\%)} = (\text{detected carbon moles in a defined product/theoretical carbon moles in product}) \times 100\%$$

3. Results and discussion

3.1. The synthesis of pyridine and 3-picoline from different carbon sources

Table 1 lists the effect of the acrolein or acetals in the condensation with ammonia over the HZSM-5 catalyst on the total yield of pyridine and 3-picoline. One can see that the total yield of pyridine and 3-picoline (Table 1, entry 1) is extremely low in the condensation of acrolein and ammonia. Simultaneously, 2-picoline and 4-picoline are not detected in the liquid-phase products (not seen here). In addition, a large amount of solid substance is generated because the polymerization of acrolein is highly significant. Namely, while acrolein is fed into the preheater, a white solid is constantly formed with increasing reaction time at the transition heat region from ambient to preheating temperature. Then, vapor acrolein is fed into the reactor. Some black solids are found on the wall of the upper part of the reactor before the feed goes into the reactor. They originate from the polymerization of acrolein. The polymers undergo decomposition under high temperature, thereby resulting in the formation of coke. Besides this, acrolein starts to appear in the gas outlet due to the catalyst deactivation by the coke, and yellow solid polymers are rapidly formed in the bottom of the reactor, which come from the polymerization of acrolein and ammonia. Meanwhile, the coke leads to a reduction the total yield of pyridine and 3-picoline, and also the lifetime of the catalysts. In this case, the formation of the solid substances blocks the feeds so that this reaction is completely restrained after running for a short time. Accordingly, it is difficult to determine the real catalytic properties of the catalysts. This nasty case is thoroughly solved when acrolein dimethyl acetal (eqn (3-1)) or acrolein diethyl acetal (eqn (3-2)) act as the starting material. The reaction schemes are as follows:

$$H_2CCHCH(OCH_3)_2 + H_2O \xleftrightarrow{\text{Catalyst}} H_2CCHCHO + CH_3OH \quad (3\text{-}1)$$

$$H_2CCHCH(OC_2H_5)_2 + H_2O \xleftrightarrow{\text{Catalyst}} H_2CCHCHO + C_2H_5OH \quad (3\text{-}2)$$

Table 1 Total yield of pyridine and 3-picoline over HZSM-5 from the condensation of different reactants[a]

Entry	Carbon sources	Pyridine	3-Picoline	Total yield	Others
1	R1	1.46%	1.74%	3.20%	96.80%
2	R2	19.70%	23.54%	43.24%	56.76%
3	R3	19.80%	18.81%	38.61%	61.39%

[a] R1: acrolein. Reaction conditions: reaction temperature = 425 °C; LHSV = 1.50 h^{-1}; molar ratio of acrolein/ammonia = 1/2; TOS = 1–2 h. Others: CO_x, 3,5-dimethylpyridine, coke, *etc.* R2: acrolein dimethyl acetal. Reaction conditions: reaction temperature = 450 °C; LHSV = 0.85 h^{-1}; molar ratio of acrolein dimethyl acetal/ammonia = 1/4; TOS = 1–3 h. Others: CO_x, 2-picoline, 3,5-dimethylpyridine, coke, *etc.* R3: acrolein diethyl acetal. Reaction conditions: reaction temperature = 450 °C; LHSV = 0.85 h^{-1}; molar ratio of acrolein diethyl acetal/ammonia = 1/4; TOS = 1–3 h. Others: CO_x, 2-picoline, 4-picoline, 3,5-dimethylpyridine, coke, *etc.*

$$H_2CCHCHO + NH_3 \xrightarrow{\text{Catalyst}} C_6H_7N\ (3\text{-picoline}) \quad (3\text{-}3)$$

The physicochemical properties of acrolein dimethyl acetal and acrolein diethyl acetal are much more stable in the absence of an acid catalyst. Polymerization does not occur before the feeds go through the catalyst. The reaction to give pyridine and 3-picoline mainly occurs from the condensation of acrolein and ammonia due to the extremely strong reactivity of acrolein relative to that of methanol or ethanol (eqn (3-3)). Accordingly, some methanol or ethanol are detected in the liquid-phase products under all the reaction conditions in this work. Even though unreacted acrolein appears, acrolein dimethyl acetal or acrolein diethyl acetal is generated from the condensation of unreacted acrolein and methanol or ethanol. Our experimental results show that these yellow polymers are easily dissolved in the methanol or ethanol. Accordingly, the problem of the polymerization is effectively solved. This analysis is further confirmed by the catalytic results showing that the yields of pyridine and 3-picoline from acetals (Table 1, entries 2 and 3) are significantly higher than that of the former (Table 1, entry 1). The above results show that acrolein is principally involved in these reactions relative to methanol or ethanol after the decomposition of acetals. Besides the role of avoiding polymerization, it is found that 4-picoline is not detected from the condensation of acrolein dimethyl acetal and ammonia. The obvious merit is that this is in favor of separation of products, since the boiling points between 3-picoline and 4-picoline are extremely close. Accordingly, this provides a novel pathway for the synthesis of 3-picoline without the generation of 4-picoline during the gas-phase synthetic method. The related study is investigated in further work. Additionally, acrolein diethyl acetal is obtained from the reaction of acrolein and ethanol, and acrolein is easily generated by the dehydration of bio-glycerol. Thus, acrolein diethyl acetal can be produced from biomass. Accordingly, this offers a sustainable pathway for the synthesis of pyridine and 3-picoline.

3.2. The synthesis of pyridine and 3-picoline from gas-phase acrolein diethyl acetal and ammonia over various catalysts

It is reported that MgF_2/Al_2O_3 is an effective catalyst in the condensation of acrolein and ammonia toward pyridine and 3-picoline.[3] Table 2 lists the effect of the MgF_2-containing catalysts on the total yield of pyridine and 3-picoline. One can see that the total yield of pyridine and 3-picoline is low for all the catalysts. Among them, the MgF_2/base Al_2O_3 catalyst (Table 2, entries 1 and 2) exhibits the highest total yield of pyridine and 3-picoline whereas the MgF_2/γ-Al_2O_3 catalyst (Table 2, entry 3) shows the worst catalytic performance. From the results it can be concluded that the total yields of pyridine and 3-picoline over MgF_2-containing catalysts are not very ideal. Accordingly, the development of a highly effective catalyst in the synthesis of pyridine and 3-picoline is desired.

Zeolites are widely applied for various kinds of reactions such as those of pyridine bases,[7–10] as they possess many advantages such as high specific surface area and strong

Table 2 Total yield of pyridine and 3-picoline from the condensation of acrolein diethyl acetal and ammonia over various catalysts[a]

Entry	Catalysts	Pyridine	3-Picoline	Total yield	Others
1	MgF_2/Al_2O_3[b]	7.85%	10.83%	18.86%	81.14%
2	MgF_2/Al_2O_3[c]	4.63%	5.84%	10.47%	89.53%
3	MgF_2/Al_2O_3[d]	0.46%	0.49%	0.95%	99.05%
4	MgF_2/Al_2O_3[e]	1.28%	1.76%	3.04%	96.96%

[a] Reaction conditions: reaction temperature = 450 °C; LHSV = 0.85 h^{-1}; molar ratio of acrolein diethyl acetal/ammonia = 1/4; TOS = 1–3 h. Others: CO_x, 2-picoline, 4-picoline, 3,5-dimethylpyridine, coke, *etc.* [b] Base Al_2O_3, content of MgF_2: 1 wt%. [c] Base Al_2O_3, content of MgF_2: 10 wt%. [d] γ-Al_2O_3, content of MgF_2: 1 wt%. [e] α-Al_2O_3, content of MgF_2: 1 wt%.

hydrothermal stability. Table 3 lists the effect of various zeolites on the total yield of pyridine and 3-picoline. One can see that the total yield of pyridine and 3-picoline over various zeolites (Table 3, entries 1–4) displays the order HZSM-5 > *X* > *Y* ≫ *A*. Obviously, the HZSM-5 catalyst gives the highest total yield of pyridine and 3-picoline, whereas the A catalyst gives the lowest total yield of pyridine and 3-picoline. The difference is attributed to the nature of the zeolites. This is due to the fact that HZSM-5 possesses a moderate pore size relative to other zeolites, which is in favor of providing shape selectivity. It is reasonable that the type of zeolite is an important factor in this reaction and this is in agreement with the literature.[1] Unless otherwise specifically mentioned, Si/Al = 25 in HZSM-5. To further improve the total yield of pyridine and 3-picoline, some active components are loaded onto HZSM-5. Table 4 lists the effect of various HZSM-5 supported catalysts on the total yield of pyridine and 3-picoline in the condensation of acrolein diethyl acetal and ammonia. It is clearly found that the total yield of pyridine and 3-picoline over the ZnO/HZSM-5 (Table 4, entry 2) catalyst is higher than that of the MgF_2/HZSM-5 (Table 4, entry 1) catalyst. This indicates that introducing ZnO is more favourable for improving the total yield of pyridine and 3-picoline in this reaction. Acidity is a key factor in the synthesis of pyridine bases.[7–11] Two promising methods can alter the acidity of the catalysts. On the one hand, it is well accepted that the acidity of HZSM-5 becomes stronger when the content of aluminum is higher. By decreasing the Si/Al ratio in HZSM-5, the total yield of pyridine and 3-picoline over the ZnO/HZSM-5 catalyst (Table 4, entry 3) is remarkably increased. One the other hand, adding acidic species to HZSM-5 can also achieve this effect. It is observed (Table 4, entries 4–7) that the total yield of pyridine and 3-picoline displays the order HF/HZSM-5 > H_2SO_4/HZSM-5 > H_3BO_3/HZSM-5 > H_3PO_4/HZSM-5. Compared with HZSM-5, only HF/HZSM-5 exhibits a higher catalytic performance. Clearly, changing the Si/Al ratio in HZSM-5 is a better alternative for improving the total yield of pyridine and 3-picoline. According to the reaction mechanisms,[11–14] dehydration and/or dehydrogenation are indispensable processes in the synthesis of pyridine bases. The possible reaction mechanisms are shown as follows (eqn (3-4) to (3-7)):

$$H_2CCHCHO + NH_3 \rightarrow H_2CCHCHNH \rightarrow C_6H_7N \quad (3\text{-}4)$$

$$H_2CCHCHO + H^{(+)} \rightarrow H_2C^{(+)}CH_2CHO \quad (3\text{-}5)$$

$$H_2C^{(+)}CH_2CHO + H_2CCHCHO \rightarrow HOCCH_2CH_2CH(CHO)CH_2 \rightarrow HOCCH_2CH_2C(CHO)CH_2 + H^{(+)} \quad (3\text{-}6)$$

$$HOCCH_2CH_2C(CHO)CH_2 + NH_3 \rightarrow C_6H_7N \text{ (3-picoline)} \quad (3\text{-}7)$$

Accordingly, the catalyst must first possess acidic sites to catalyze this reaction. It is well-known that solid base is an effective dehydrogenation catalyst.[15] However, it is found that the total yield of pyridine and 3-picoline decreased when introducing a strong base such as KF into HZSM-5 (Table 4, entries 8 and 9). From the results it can be concluded that the catalytic performance is strongly dependent on the acidity of HZSM-5. Adding ZnO to HZSM-5 can accelerate the dehydrogenation to reduce the hydrogen migration. It is well known that strong solid acid and strong solid base can readily activate the polymerization of acrolein, thereby resulting in a loss of catalytic performance. Therefore, the total yield of pyridine and 3-picoline over ZnO/HZSM-5 is improved, but the total yields of pyridine and 3-picoline over H_2SO_4/HZSM-5 and KF/HZSM-5 are both decreased. Additionally, it is observed that the total yields of pyridine and 3-picoline over the bi-metal oxide-containing catalysts (Table 4, entries 10–13) are decreased relative to that of ZnO/HZSM-5 alone (Table 4, entry 3). This is attributed to the reduction in specific surface area and acidity.

Alkaline–acid sequential treatment usually enhances the stability of catalysts in some reactions.[16,17] For example, Jin *et al.*[16] reported that the yield of pyridine and the stability are increased when HZSM-5 is treated with alkaline solution. Table 5 lists the effect of various catalysts prepared by alkaline treatment and alkaline–acid sequential treatment on the total yield of pyridine and 3-picoline. One can see that the total yield of pyridine and 3-picoline over the treated HZSM-5 catalysts is no more than 38% (Table 5, entries 1 and 2). This indicates that alkali-treated and/or alkaline–acid sequentially-treated HZSM-5 can not improve the total yield of pyridine and 3-picoline. A similar change in the total yield of pyridine and 3-picoline is exhibited when using ZnO-containing catalysts (Table 5, entries 3 and 4). Meanwhile, the total yield of pyridine and 3-picoline for the ZnO catalysts (Table 4, entry 3; Table 5, entries 3 and 4) is greatly improved relative to the corresponding parent catalysts

Table 3 Total yield of pyridine and 3-picoline from the condensation of acrolein diethyl acetal and ammonia over various catalysts[a]

Entry	Catalysts	Pyridine	3-Picoline	Total yield	Others
1	HZSM-5	19.81%	18.80%	38.61%	61.39%
2	Y	10.72%	16.96%	27.68%	72.32%
3	X	8.22%	20.26%	28.48%	71.52%
4	A	1.03%	0.13%	1.16%	98.84%

[a] Reaction conditions: reaction temperature = 450 °C; LHSV = 0.85 h^{-1}; molar ratio of acrolein diethyl acetal/ammonia = 1/4; TOS = 1–3 h. Others: CO_x, 2-picoline, 4-picoline, 3,5-dimethylpyridine, coke, *etc.*

Table 4 Total yield of pyridine and 3-picoline from the condensation of acrolein diethyl acetal and ammonia over various catalysts[a]

Entry	Catalysts	Pyridine	3-Picoline	Total yield	Others
1	MgF_2/HZSM-5[b]	15.21%	16.55%	31.76%	68.24%
2	ZnO/HZSM-5[b]	13.51%	23.50%	37.01%	62.99%
3	ZnO/HZSM-5	26.87%	34.27%	61.14%	38.86%
4	H_2SO_4/HZSM-5	9.89%	15.57%	25.46%	74.54%
5	H_3BO_3/HZSM-5	10.54%	10.01%	20.54%	79.46%
6	H_3PO_4/HZSM-5	1.71%	1.67%	3.38%	96.62%
7	HF/HZSM-5	17.44%	23.16%	40.60%	79.46%
8	KF/HZSM-5	14.72%	21.87%	36.59%	63.41%
9	LaF_3/HZSM-5	14.98%	21.60%	36.58%	63.42%
10	$Fe_{0.5}Zn_{1.0}O_x$/HZSM-5	20.49%	26.07%	46.56%	53.44%
11	$Co_{0.5}Zn_{1.0}O_x$/HZSM-5	19.67%	28.77%	48.44%	51.56%
12	$Ni_{0.5}Zn_{1.0}O_x$/HZSM-5	21.47%	29.01%	50.48%	49.52%
13	$Mo_{0.5}Zn_{1.0}O_x$/HZSM-5	20.74%	21.98%	42.72%	57.28%

[a] Reaction conditions: reaction temperature = 450 °C; LHSV = 0.85 h^{-1}; molar ratio of acrolein diethyl acetal/ammonia = 1/4; TOS = 1–3 h. Others: CO_x, 2-picoline, 4-picoline, 3,5-dimethylpyridine, coke, *etc.* [b] HZSM-5: Si/Al = 80.

(Table 3, entry 1; Table 5, entries 1 and 2). It is reasonable that ZnO improves the series of HZSM-5 catalysts (total yield <0.5% for pure ZnO catalyst). In terms of the ZnO/HZSM-5 (Table 4, entry 3) and ZnO/HZSM-5-At-acid (Table 5, entry 4) catalysts, it has a greater effect on the product distribution, although it hardly affects the total yield of pyridine and 3-picoline. This is in agreement with the literature.[12] When increasing the Si/Al ratio (Table 5, entry 5), the total yield of pyridine and 3-picoline is decreased. This shows that the newly formed hierarchical structure in HZSM-5 caused by alkaline treatment may have a negative effect on the total yield of pyridine and 3-picoline. This is due to the fact that a larger pore size is formed during alkaline treatment when the Si/Al ratios in HZSM-5 are above 50.[18] In contrast, the ZnO/HZSM-5-At-acid catalyst (Table 5, entry 7) exhibits a higher total yield of pyridine and 3-picoline than the ZnO/HZSM-5 catalyst (Table 5, entry 6) in the condensation of acrolein dimethyl acetal and ammonia. Besides this, a low total yield of pyridine and 3-picoline over the ZnO/HZSM-5-At-acid catalyst (Table 5, entry 8) is obtained from the reaction of ethanol and ammonia. Obviously, the effect of ethanol from the decomposition of acrolein diethyl acetal on the ZnO/HZSM-5-At-acid catalyst is limited. This may enhance the stability of the catalysts by weakening the polymerization of acrolein. In a word, the ZnO/HZSM-5-At-acid catalyst shows a satisfactory total yield of pyridine and 3-picoline relative to other catalysts with various reactants in this work.

Fig. 1 shows the effect of the time on stream (TOS) on the total yield of pyridine and 3-picoline over the ZnO/HZSM-5 and ZnO/HZSM-5-At-acid catalysts. One can see that the total yield of pyridine and 3-picoline over the ZnO/HZSM-5-At-acid catalyst slowly decreased over the course of 50 h. In contrast, the total yield of pyridine and 3-picoline over the ZnO/HZSM-5 catalyst is remarkably reduced at TOS = 0–11 h. From the results it can be concluded that ZnO/HZSM-5-At-acid can enhance not only the total yield of pyridine and 3-picoline but also the catalyst stability. Recent studies reveal that Zn species on ZSM-5 are responsible for the stability in some applications, although ZSM-5 is only treated with alkaline solution. Li *et al.*[19] suggested that the distance between Zn sites and acid sites in ZSM-5 was effectively shortened, which led to the intermediates being faster to access the Zn sites through dehydrogenation. Thus, the steric effect for the micropores was diminished. Ni *et al.*[20] considered that Zn species not only catalyzed the dehydrogenation of alkanes and alkenes, but also increased the rate of recombinative desorption of the hydrogen atoms formed in C–H activation steps.

Table 5 Total yield of pyridine and 3-picoline over various catalysts[a]

Entry	Carbon sources	Catalysts	Pyridine	3-Picoline	Total yield	Others
1	R3	HZSM-5-At	17.14%	17.64%	34.78%	65.22%
2	R3	HZSM-5-At-acid	17.23%	20.28%	37.48%	62.52%
3	R3	ZnO/HZSM-5-At	27.44%	25.90%	53.34%	46.66%
4	R3	ZnO/HZSM-5-At-acid	31.77%	29.24%	61.01%	38.99%
5	R3	ZnO/HZSM-5-At-acid[b]	19.13%	26.12%	45.25%	54.75%
6	R2	ZnO/HZSM-5	22.25%	23.69%	45.94%	54.06%
7	R2	ZnO/HZSM-5-At-acid	29.24%	26.12%	55.36%	44.64%
8	R4	ZnO/HZSM-5-At-acid	5.58%	0.76%	6.34%	93.66%

[a] R2: acrolein dimethyl acetal; R3: acrolein diethyl acetal; R4: ethanol. Reaction conditions: reaction temperature = 450 °C; LHSV = 0.85 h^{-1}; molar ratio of acrolein diethyl acetal/ammonia = 1/4; TOS = 1–3 h. Others: CO_x, 2-picoline, 3,5-dimethylpyridine, coke, *etc.* [b] Before alkaline treatment HZSM-5: Si/Al = 100.

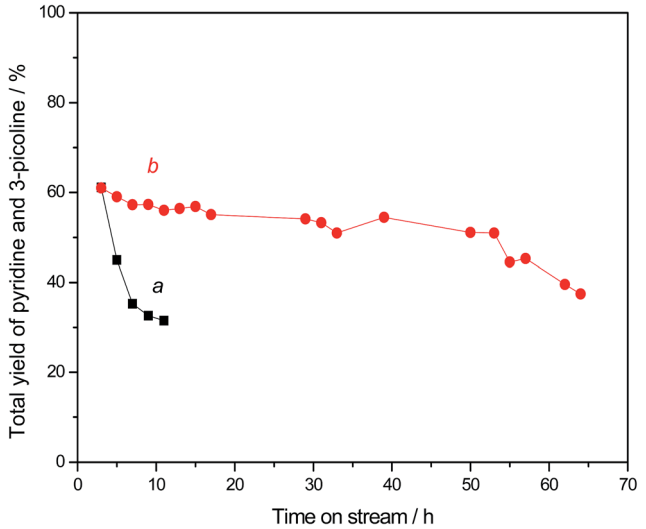

Fig. 1 The stability of various catalysts as a function of time. (a) ZnO/HZSM-5; (b) ZnO/HZSM-5-At-acid. Reaction conditions: reaction temperature = 450 °C; LHSV = 0.85 h^{-1}; molar ratio of acrolein diethyl acetal/ammonia = 1/4.

3.3. Characterization

Fig. 2 shows the XRD patterns of the HZSM-5, HZSM-5-At, HZSM-5-At-acid, ZnO/HZSM-5 and ZnO/HZSM-5-At-acid catalysts. One can see that the XRD patterns of all the catalysts exhibit the characteristic peaks of HZSM-5, hinting that the original structure of HZSM-5 is almost retained after alkaline treatment or alkaline–acid sequential treatment or when supporting ZnO. For the non-ZnO-containing catalysts, it is observed that the position of the diffraction peaks in the HZSM-5-At catalyst is slightly shifted to a higher angle. This shows that the degree of desilication is very small and dealumination also occurred during treatment. Moreover, the intensity of the strongest diffraction peak in the HZSM-5-At catalyst is decreased. This indicates that the crystallinity of the catalyst is reduced due to the removal of some species from the framework of the HZSM-5 catalyst. Fig. 3 shows the ^{27}Al MAS NMR spectrum of the HZSM-5 and HZSM-5-At catalysts. Generally, a peak at about 50 ppm for the zeolites represents the framework aluminum species and at about 0 ppm represents the extra-framework aluminum species. Only one peak at about 50 ppm is observed for the HZSM-5 catalyst, showing that all the aluminum species are located in the framework of the catalyst. After alkaline treatment, two peaks at about 50 ppm and 0 ppm are clearly observed for the HZSM-5-At catalyst. This shows that dealumination has happened to generate the extra-framework

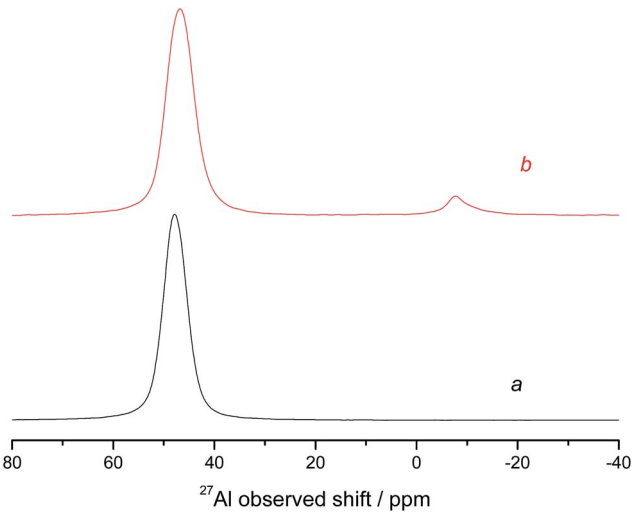

Fig. 3 ^{27}Al MAS NMR for various catalysts. (a) HZSM-5; (b) HZSM-5-At.

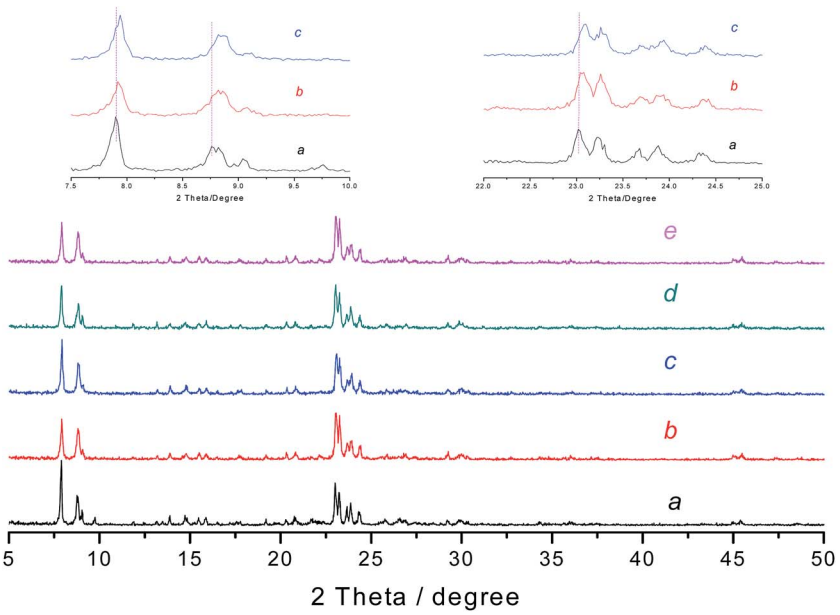

Fig. 2 XRD patterns for various catalysts. (a) HZSM-5; (b) HZSM-5-At; (c) HZSM-5-At-acid; (d) ZnO/HZSM-5; (e) ZnO/HZSM-5-At-acid.

aluminum species. Much literature[6,17,18] has reported that the behaviors of desilication and dealumination occurred during alkaline treatment. This is strongly dependent on the Si/Al ratio (mol mol^{-1}) in HZSM-5. The authors considered that the framework aluminum controlled the process of framework silicon extraction and made desilication selective towards the formation of intracrystalline mesopores. At lower Si/Al ratios, the relatively high alumina content inhibited silicon extraction and any mesopores were hardly created. However, the unselective extraction of framework silicon species induced the formation of a larger pore size in highly siliceous ZSM-5. A substantial number of aluminum species were generated on the surface of zeolites during alkaline treatment, and acid-washing was an effective method.[21,22] After acid washing the HZSM-5-At catalyst, the diffraction peaks in the HZSM-5-At-acid catalyst continue to shift toward a higher angle. This shows that the distance between atoms in the framework of the HZSM-5-At-acid catalyst becomes shorter due to the removal of alumina species. Simultaneously, the intensity of the strongest diffraction peak is to some extent restored, implying that some surface species are removed. The literature[6] has reported that the newly generated aluminum species during alkaline treatment had a negative influence on the catalytic performance. Removal of these extra-framework aluminum species by acid washing can enhance the catalytic performance. This is in agreement with the catalytic results in this work. For the ZnO-containing catalyst, the diffraction peaks for ZnO are not observed ($2\theta = 31.1°$, 34.1°, 36.1° and 56.2°) in the ZnO/HZSM-5 and ZnO/HZSM-5-At-acid catalysts. This shows that ZnO particles are highly dispersed on the supports. This is due to the fact that the ZnO particles are too small as a result of the low Zn loading, so that it is not observed beyond the XRD instrument. The intensity of the diffraction peaks of the various catalysts displays the order ZnO/HZSM-5 > ZnO/HZSM-5-At-acid. This further confirms that some surface species are still retained on the HZSM-5-At-acid catalyst.

Fig. 4 shows the XPS profiles of the various elements in the ZnO/HZSM-5, ZnO/HZSM-5-At and ZnO/HZSM-5-At-acid catalysts. For Zn $2p_{1/2}$ and Zn $2p_{3/2}$, one can see that the binding energies of Zn $2p_{1/2}$ and Zn $2p_{3/2}$ in the ZnO/HZSM-5 catalyst are 1045.9 eV and 1022.8 eV, respectively, which are slightly higher than that of bulk ZnO (1045.0 eV and 1022.0 eV, respectively). This shows that the most common valence state of the Zn is +2. Both the ZnO/HZSM-5-At and ZnO/HZSM-5-At-acid catalysts show the BE of Zn $2p_{3/2}$ at 1023.3 eV. Also, the BE values for Zn $2p_{1/2}$ are displayed at 1045.8 eV and 1046.6 eV, respectively. Obviously, the alkaline treatment and alkaline–acid sequential treatment had little effect on the chemical nature of ZnO. Nevertheless, the BE value of Zn $2p_{1/2}$ in the ZnO/HZSM-5-At-acid catalyst is higher than that of the ZnO/HZSM-5 and ZnO/HZSM-5-At catalysts. This shows that the interaction between ZnO and the support became stronger. For O 1s, the BE value in the ZnO/HZSM-5 catalyst is 532.4 eV and the corresponding values in the ZnO/HZSM-5-At and ZnO/HZSM-5-At-acid catalysts are both 532.7 eV. This indicates that absorbed oxygen species other than ZnO appear on the surface of the supports. The BE values in the treated catalysts become larger, demonstrating that more oxygen species are adsorbed. This is in agreement with the change in the BE of Zn. In terms of Si 2p, the binding energy in the ZnO/HZSM-5 catalyst is observed at 102.9 eV. This value is increased to 103.3 eV, pointing to the Si^{4+} peak for the ZnO/HZSM-5-At and ZnO/HZSM-5-At-acid catalysts, hinting that the thickness increases in the form of oxides. These oxides are derived from the selective removal of silicon from the framework of the zeolites during desilication. Thus, they are retained on the surface of the alkali-treated catalyst, and meanwhile, this shows that acid washing the alkali-treated catalyst has no influence on these oxides. Nevertheless, the change in the aluminum species is difference. The evidences are that the BE of Al 2p in the ZnO/HZSM-5-At-acid catalyst becomes smaller than that of the ZnO/HZSM-5-At one. Simultaneously, their values for both the catalysts are larger, showing that dealumination occurred during alkaline treatment or alkaline–acid sequential treatment. It is reasonable that alkaline treatment and alkaline–acid sequential treatment have important influences on the various elements in the ZnO/HZSM-5-At and ZnO/HZSM-5-At-acid catalysts relative to the ZnO/HZSM-5 catalyst, and the acid washing process mainly has an effect on the Zn and Al species.

Fig. 5 shows the UV-vis DRS spectra of the ZnO/HZSM-5 and ZnO/HZSM-5-At-acid catalysts. Three absorption bands at about 220 nm, 270 nm and 368 nm are observed for the ZnO/HZSM-5 catalyst, and meanwhile, two absorption bands at about 220 nm and 270 nm are clearly seen for the ZnO/HZSM-5-At-acid catalyst. The band at about 368 nm is attributed to the ZnO particles, which are distributed on the external surface of the zeolites.[23] The band at about 270 nm is attributed to the ZnO clusters of about 1 nm,[23] which are distributed in the channels of the zeolites. The band at about 220 nm is derived from the interaction of more strongly electron conducting groups than the O^{2-} group. Accordingly, the form of ZnO in the ZnO/HZSM-5-At-acid catalyst is mainly ZnO clusters, and more ZnO particles appear on the external surface of the ZnO/HZSM-5 catalyst.

Table 6 lists the texturalproperties of the HZSM-5, HZSM-5-At, HZSM-5-At-acid, ZnO/HZSM-5 and ZnO/HZSM-5-At-acid catalysts. One can see that the specific surface areas of the various catalysts display the order HZSM-5-At-acid > HZSM-5 > HZSM-5-At and the external surface areas of the various catalysts display the order HZSM-5-At-acid > HZSM-5-At > HZSM-5. This indicates that alkaline–acid sequential treatment is favourable in increasing the specific surface area and the external surface area. The lowest specific surface area for the HZSM-5-At catalyst is attributed to the depositions covering or blocking the pore channels during alkaline treatment. This is very consistent with the ^{27}Al MAS NMR and XRD results. By acid washing, the specific surface area of the HZSM-5-At-acid catalyst is remarkably increased relative to the HZSM-5 and HZSM-5-At catalysts. This is due to the fact that some depositions are removed after acid washing. In addition, it is observed that the mesopore volumes in the alkali-treated and alkali–acid sequentially-treated catalysts are both increased relative to the parent catalyst. When introducing ZnO into HZSM-5 and HZSM-5-At-acid catalysts, the micropore surface areas of the ZnO/HZSM-5 and ZnO/HZSM-5-At-acid catalysts are both decreased

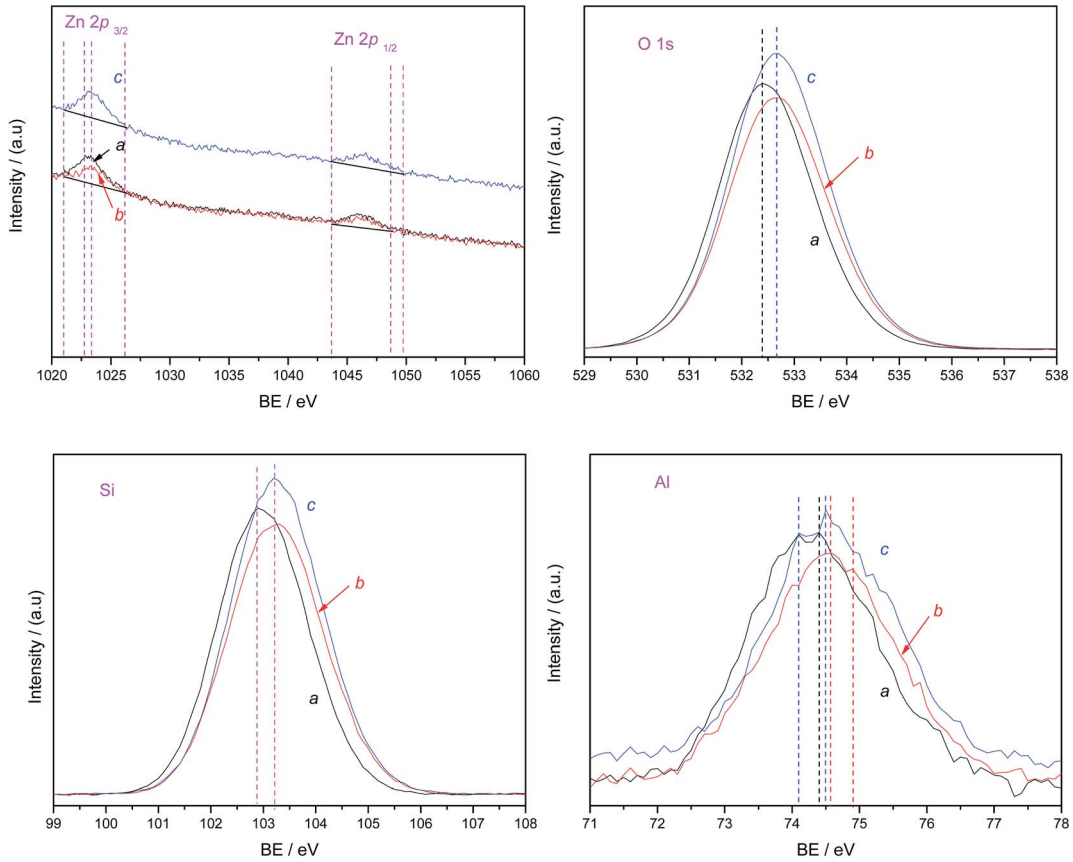

Fig. 4 XPS profiles for various catalysts. (a) ZnO/HZSM-5; (b) ZnO/HZSM-5-At; (c) ZnO/HZSM-5-At-acid.

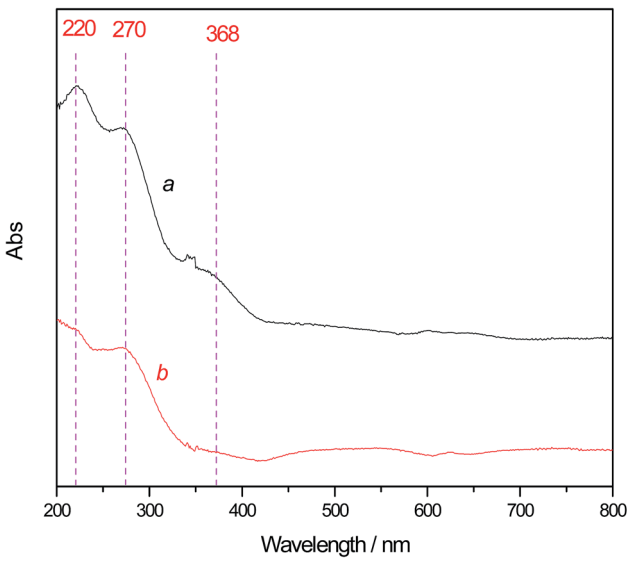

Fig. 5 UV-vis DRS spectra for various catalysts. (a) ZnO/HZSM-5; (b) ZnO/HZSM-5-At-acid.

relative to the parent catalysts, which are partially occupied by Zn, during the preparation of ZnO-containing catalysts. The external surface area of the ZnO/HZSM-5-At-acid catalyst is slightly decreased relative to the HZSM-5-At-acid catalyst, showing that most of the ZnO is in the form of clusters which are located in the HZSM-5-At-acid. Nevertheless, the external surface area of the ZnO/HZSM-5 catalyst is increased relative to the HZSM-5 catalyst, which is attributed to the intercrystalline space between particles because more ZnO particles are distributed on the external surface area. This is in agreement with the UV-vis DRS results. Fig. 6 shows the N_2 adsorption–desorption of the HZSM-5, HZSM-5-At, HZSM-5-At-acid, ZnO/HZSM-5 and ZnO/HZSM-5-At-acid catalysts. All the catalysts demonstrate I-type isotherms with a steep slope at low relative pressure, showing the existence of micropores. However, a hysteresis at relative higher pressures is not clearly observed, implying that a limited hierarchical structure is obtained. This is further confirmed by the pore distribution of the ZnO/HZSM-5-At-acid catalyst shown in Fig. 7.

Fig. 8 shows the NH_3-TPD profiles of the HZSM-5, HZSM-5-At, HZSM-5-At-acid, ZnO/HZSM-5 and ZnO/HZSM-5-At-acid catalysts. Two desorption peaks can be identified from the profiles, and the temperature at maximum ($T_{m,i}$) and integral area (A_i) of the peaks, which correspond respectively to the strength and concentration of acid sites, are summarized in Table 7. One can see that the $T_{m,1}$ peak at 100–300 °C is present for all the catalysts, and this peak can be assigned to the weakly acidic sites.[24,25] The $T_{m,2}$ peak at above 300 °C is present for all the catalysts, and this peak can be assigned to the strongly acidic sites.[24,25] For the non-ZnO-containing catalysts, the total

Table 6 Textural properties of various catalysts[a]

Catalysts	S_{BET} ($m^2\ g^{-1}$)	S_{micro} ($m^2\ g^{-1}$)	S_{ext} ($m^2\ g^{-1}$)	V_{total} ($cm^3\ g^{-1}$)	V_{micro} ($cm^3\ g^{-1}$)	V_{meso} ($cm^3\ g^{-1}$)
HZSM-5	336.5	304.4	32.1	0.2121	0.1348	0.0773
HZSM-5-At	309.8	247.6	62.2	0.2447	0.1294	0.1183
HZSM-5-At-acid	380.9	292.1	88.8	0.3090	0.1316	0.1774
ZnO/HZSM-5	336.8	299.1	37.7	0.2235	0.1243	0.0992
ZnO/HZSM-5-At-acid	372.1	284.6	87.5	0.3256	0.1273	0.1983

[a] Note: S_{BET}, S_{micro} and S_{ext} refer to specific surface area, micropore surface area and external surface area, respectively, and $S_{BET} = S_{micro} + S_{ext}$; V_{total}, V_{micro} and V_{meso} refers to total pore volume, micropore volume and mesopore volume, respectively, and $V_{total} = V_{micro} + V_{meso}$.

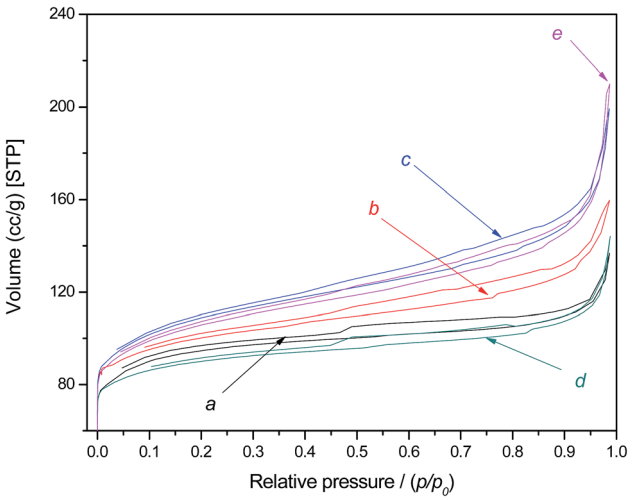

Fig. 6 N_2 adsorption–desorption isotherms for various catalysts. (a) HZSM-5; (b) HZSM-5-At; (c) HZSM-5-At-acid; (d) ZnO/HZSM-5; (e) ZnO/HZSM-5-At-acid.

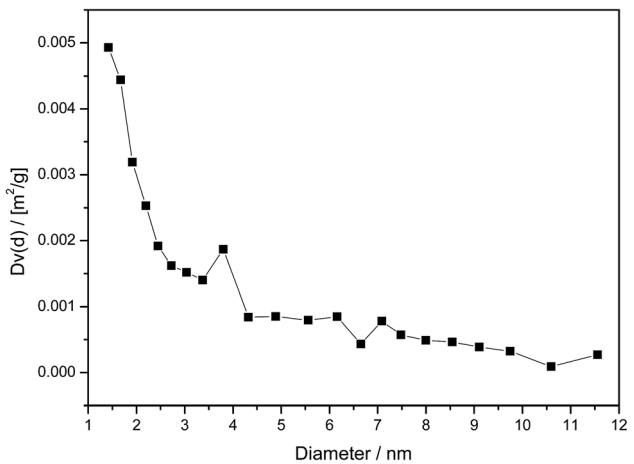

Fig. 7 The pore size distribution of the ZnO/HZSM-5-At-acid catalyst.

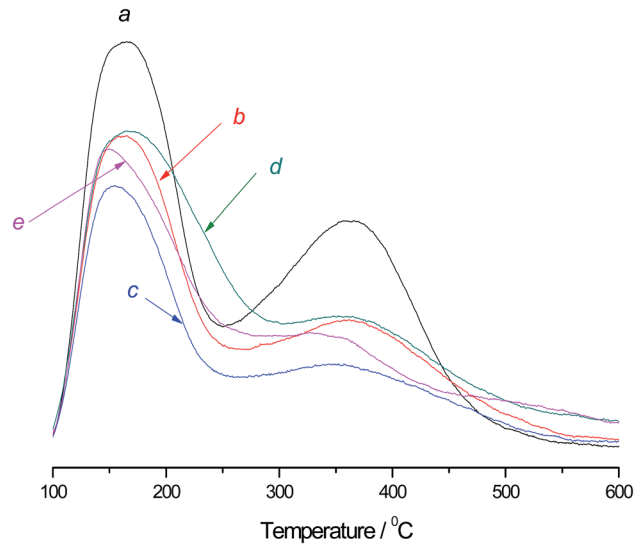

Fig. 8 NH_3-TPD profiles for various catalysts. (a) HZSM-5; (b) HZSM-5-At; (c) HZSM-5-At-acid; (d) ZnO/HZSM-5; (e) ZnO/HZSM-5-At-acid.

concentration of the acidic sites over various catalysts displays the order HZSM-5 > HZSM-5-At > HZSM-5-At-acid. This is due to the fact that there are interactions of weakly acidic sites and strongly acidic sites with alkaline and acid solutions. For the ZnO-containing catalysts, the total concentration of the acidic sites displays the order ZnO/HZSM-5 > ZnO/HZSM-5-At-acid, which is the same order as for the parent catalysts. Meanwhile, it is observed that the total concentration of the ZnO/HZSM-5-At-acid catalyst is increased but the total concentration of the ZnO/HZSM-5 catalyst is decreased relative to that of the corresponding to the parent catalysts. It is found that the concentrations of the weakly acidic sites in the two supported catalysts are increased, which is attributed to the nature of ZnO. In any event, the concentration of the weakly acidic sites is higher than that of the strongly acidic sites, implying that the weakly acidic sites mainly act as the catalytically active sites in the these reactions. The types of acidic sites are investigated in further work.

The literature[26–28] on ZnO/HZSM-5 catalysts made using the wet-impregnation method showed that the most probably formed zinc species was $ZnOH^+$, which was from the interaction between ZnO and acid sites ($ZnO + H^+ \rightarrow ZnOH^+$); however, it was unstable under high temperature treatment, and ($O–Zn^{2+}–O$) or ($Zn^{2+}–O–Zn^{2+}$) species were generated according to the Zn loading in the ZnO/HZSM-5 catalyst.[26] At low Zn loading (<1.3 wt%), ($O–Zn^{2+}–O$) species were formed during the preparation of the ZnO/HZSM-5 catalyst, resulting in decreasing acidity relative to the HZSM-5 catalyst; At high Zn loading (>1.3 wt%), ($Zn^{2+}–O–Zn^{2+}$) species were generated by the interaction

Table 7 NH_3-TPD results of various catalysts

	$T_{m,i}$[a] and A_i[b] for various desorption peaks				
Catalysts	$T_{m,1}$ (°C)	A_1 (mmol g^{-1})	$T_{m,2}$ (°C)	A_2 (mmol g^{-1})	A_{total} (mmol g^{-1})
HZSM-5	165.2	0.8394	365.8	0.7875	1.6269
HZSM-5-At	165.6	0.6836	362.4	0.4804	1.1640
HZSM-5-At-acid	154.6	0.5818	352.3	0.3621	0.9439
ZnO/HZSM-5	167.8	0.9416	353.7	0.5248	1.4664
ZnO/HZSM-5-At-acid	150.7	0.7465	325.7	0.4545	1.2010

[a] $T_{m,i}$ refers to the temperature at the maximum of desorption peak i. [b] A_i refers to the integral area of desorption peak i, and it also means the concentration of acid sites corresponding to the desorption peak i; A_{total} stands for the sum of the concentrations of various acid sites, *i.e.*, $A_{total} = \Sigma A_i$.

between two $ZnOH^+$ species and the acidity of the ZnO/HZSM-5 catalyst was almost same as that of the HZSM-5 catalyst. The characterization results from Fig. 8 and Table 7 show that the acidity is decreased in the ZnO/HZSM-5 catalyst relative to the HZSM-5 catalyst. Also, the ZnO/HZSM-5 catalyst possesses low Zn loading (Zn: 1 wt%) in this work. Accordingly, (O–Zn^{2+}–O) species are formed in the ZnO/HZSM-5 catalyst in terms of the characterization results (XPS and NH_3-TPD) in this work. However, the analysis from the literature[26] is not in favor of the ZnO/HZSM-5-At-acid catalyst, since the acidity of the ZnO/HZSM-5-At-acid catalyst is increased relative to the support. This is due to the fact that the new species are created during the preparation of the ZnO/HZSM-5-At-acid catalyst and thus it enhances the acidity of the ZnO/HZSM-5-At-acid catalyst. These newly generated species during the preparation of the ZnO/HZSM-5-At-acid catalyst may be $ZnAlO_2$, from the reaction between ZnO and the extra-framework species, *i.e.* aluminum, on the surface of the HZSM-5-At-acid catalyst. It should be that the $ZnAlO_2$ catalyst possesses a stronger acidity than the ZnO catalyst. Accordingly, the acidity is increased when ZnO is added to the surface of HZSM-5-At-acid. Besides this, hydrogen is often generated in the synthesis of pyridine bases and then $ZnOH^+$ and ZnH^+ species are obtained. It is reasonable that several zinc species play crucial roles in this reaction.

In order to study the anti-coking ability of the ZnO/HZSM-5 and ZnO/HZSM-5-At-acid catalysts, we investigated the combustion behavior of coke using the TG-DSC profiles, as displayed in Fig. 9. One can see that the rate of weight loss in the used ZnO/HZSM-5-At-acid catalyst is lower than that of the used ZnO/HZSM-5 catalyst, implying that the former possesses a stronger anti-coking ability by reducing the deposition of carbon. Furthermore, the temperature for completely burning coke over ZnO/HZSM-5-At-acid becomes lower relative to ZnO/HZSM-5. These results tell us that the combustion of the deposited coke produced from the treated catalyst is easier than that from the untreated one. If the amounts and properties of the formed coke on the ZnO/HZSM-5 catalyst are almost the same as that on the ZnO/HZSM-5-At-acid catalyst, it is reasonable to infer that part of the coke is formed on the newly created external surface area of the ZnO/HZSM-5-At-acid catalyst. Thus, channel blockage by the formed coke during the synthesis of pyridine and 3-picoline is reduced.

3.4. The relationship between catalytic performance and the structure of the catalysts

Based on the catalytic performance evaluation, some useful results are obtained. In the condensation of acrolein diethyl acetal and ammonia as an example, it is determined that the total yield of pyridine and 3-picoline displays the order ZnO/HZSM-5 > ZnO/HZSM-5-At-acid. The NH_3-TPD results show that the same order as that for the total yield of pyridine and 3-picoline is displayed for the total concentration of acidic sites. Accordingly, the increase in the total concentration of acidic sites promotes the generation of pyridine and 3-picoline. It is found that the stability displays the order ZnO/HZSM-5-At-acid > ZnO/HZSM-5. The N_2-physisorption experiment shows that the same order as that for the stability is displayed for the external surface area and mesopore volume. The NH_3-TPD results show that the opposite order to that for the total yield of pyridine and 3-picoline is displayed for the total concentration of acidic sites. The decrease in the total concentration of acidic sites can reduce the formation of coke, and the increase in the external surface area and mesopore volume can accommodate

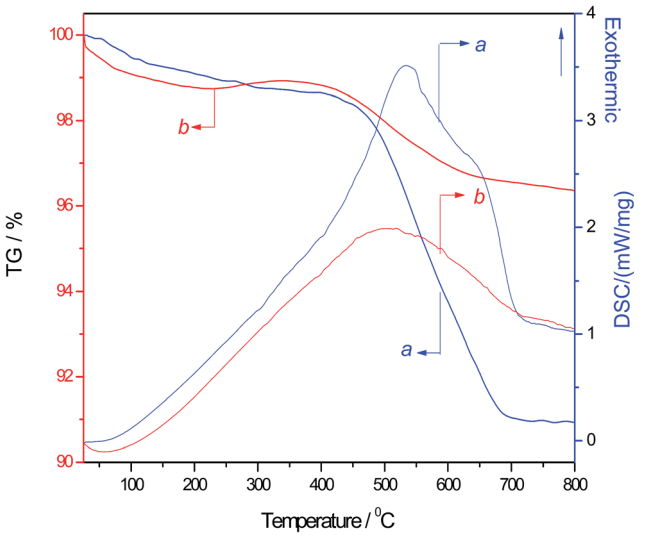

Fig. 9 TG-DSC profiles for the used catalysts with the same reaction time. (a) ZnO/HZSM-5; (b) ZnO/HZSM-5-At-acid.

more of the coke. Accordingly, the increase in the external surface area and mesopore volume and the decrease in the total concentration of acidic sites promote the stability of the catalysts. In addition, more ZnO clusters are formed in the channels of HZSM-5-At-acid. This is due to the fact that HZSM-5-At-acid can provide a more developed pore system during the preparation of the ZnO/HZSM-5-At-acid catalyst. Thus, this leads to a shorter distance between the reactants and the active sites, thereby resulting in acceleration of the reaction rates. Accordingly, pore structure, acidity and ZnO location are important factors for the synthesis of pyridine and 3-picoline in this reaction.

4. Conclusion

In summary, a novel approach for the synthesis of pyridine and 3-picoline was developed in this paper. This novel method could effectively avoid the polymerization of acrolein. Using acrolein dimethyl acetal as a model reaction, 4-picoline was not found in the liquid-phase products, making the separation of products easier. Using acrolein diethyl acetal as the raw material offered a sustainable method for the synthesis of pyridine and 3-picoline. It was found that the ZnO-containing catalysts exhibited better catalytic activity than other catalysts in this work. The stability of the ZnO/HZSM-5-At-acid catalyst was remarkably higher than that of the ZnO/HZSM-5 catalyst. The characterization revealed that the ZnO/HZSM-5-At-acid catalyst possessed a larger external surface area and mesopore volume, less acidity and more ZnO clusters located in the channels of HZSM-5-At-acid relative to the ZnO/HZSM-5 catalyst, thereby leading to longer stability.

Acknowledgements

This work was supported by the National Natural Science Foundation of China (Grant. no. 21376068), Program for New Century Excellent Talents in University, the Ministry of Education of P. R. China, and the Program for Fu-Rong Scholar in Hunan Province, P. R. China.

References

1 S. Shimizu, A. Nobuyuki, A. Iguchi and H. Sato, Synthesis of pyridine bases: general methods and recent advances in gas phase synthesis over ZSM-5 zeolite, *Catal. Surv. Jpn.*, 1998, **2**, 71–76.

2 K. R. S. K. Reddy, I. Sreedhar and K. V. Raghavan, Interrelationship of process parameters in vapor phase pyridine synthesis, *Appl. Catal., A*, 2008, **339**, 15–20.

3 H. Beschke, H. Schaefer, G. Schreyer, W. A. Schuler and W. Weigert, Catalyst for the production of pyridine and 3-methylpyridine, *US Patent*, 3,960,766, 1976.

4 H. Beschke and H. Friedrich, Process for the production of pyridine and 3-methylpyridine, *US Patent*, 4,147,874, 1979.

5 H. Beschke and H. Friedrich, Process for the production of 3-methylpyridine, *US Patent*, 4,163,854, 1979.

6 C. Fernandez, I. Stan, J. P. Gilson, K. Thomas, A. Vicente, A. Bonilla and J. Pérez-Ramírez, Hierarchical ZSM-5 zeolites in shape-selective xylene isomerization: role of mesoporosity and acid site speciation, *Chem.–Eur. J.*, 2010, **16**, 6224–6233.

7 H. Sato, S. Shimizu, N. Abe and K. I. Hirose, Vapor phase synthesis of pyridine bases from aldehydes and ammonia over pentasil zeolites, *Stud. Surf. Sci. Catal.*, 1994, **84**, 1951–1958.

8 R. R. Rao, S. J. Kulkarn, M. Subrahmanyam and A. V. R. Rao, Synthesis of pyridine and picolines over modified silica-alumina and ZSM-5 catalysts, *React. Kinet. Catal. Lett.*, 1995, **56**, 301–309.

9 A. V. Rao, S. J. Kulkarni, R. R. Rao and M. Subrahmanyam, Synthesis of 2-picoline from acetone over modified ZSM-5 catalysts, *Appl. Catal., A*, 1994, **111**, Ll0l–L108.

10 F. J. Van Der Gaag, F. Louter, J. C. Oudejans and H. V. Bekkum, Reaction of ethanol and ammonia to pyridines over zeolite ZSM-5, *Appl. Catal.*, 1986, **26**, 191–201.

11 B. Singh, S. K. Roy, K. P. Sharma and T. K. Goswami, Role of acidity of pillared inter-layered clay (PILC) for the synthesis of pyridine bases, *J. Chem. Technol. Biotechnol.*, 1998, **71**, 246–252.

12 J. R. Calvin, R. D. Davis and C. H. McAteer, Mechanistic investigation of the catalyzed vapor-phase formation of pyridine and quinoline bases using $^{13}CH_2O$, $^{13}CH_3OH$, and deuterium-labeled aldehydes, *Appl. Catal., A*, 2005, **285**, 1–23.

13 S. E. Golunski and D. Jackson, Heterogeneous conversion of acyclic compounds to pyridine bases – A review, *Appl. Catal.*, 1986, **23**, l–14.

14 Y. Higashio and T. Shoji, Heterocyclic compounds such as pyrrole, pyridines, pyrrolidine, piperidine, indole, imidazol and pyrazines, *Appl. Catal., A*, 2004, **260**, 251–259.

15 A. Music, J. Batista and J. Levec, Gas-phase catalytic dehydrogenation of methanol to formaldehyde over ZnO/SiO_2 based catalysts, zeolites, and phosphates, *Appl. Catal., A*, 1997, **165**, 115–131.

16 F. Jin, Y. Tian and Y. D. Li, Effect of alkaline treatment on the catalytic performance of ZSM-5 catalyst in pyridine and picolines synthesis, *Ind. Eng. Chem. Res.*, 2009, **48**, 1873–1879.

17 M. Ogura, S. Shinomiya, J. Tateno, Y. Nara, M. Nomura, E. Kikuchi and M. Matsukata, Alkali-treatment technique – New method for modification of structural and acid-catalytic properties of ZSM-5 zeolites, *Appl. Catal., A*, 2001, **219**, 33–43.

18 J. C. Groen, J. A. Moulijn and J. Pérez-Ramírez, Alkaline post treatment of MFI zeolites. From accelerated screening to scale-up, *Ind. Eng. Chem. Res.*, 2007, **46**, 4193–4201.

19 Y. N. Li, S. L. Liu, S. J. Xie and L. Y. Xu, Promoted metal utilization capacity of alkali-treated zeolite: preparation of Zn/ZSM-5 and its application in 1-hexene aromatization, *Appl. Catal., A*, 2009, **360**, 8–16.

20 Y. M. Ni, A. M. Sun, X. L. Wu, G. L. Hai, J. L. Hu, T. Li and G. X. Li, Preparation of hierarchical mesoporous Zn/HZSM-

5 catalyst and its application in MTG reaction, *J. Nat. Gas Chem.*, 2011, **20**, 237–242.

21 P. Sazama, B. Wichterlova, J. Dedecek, Z. Tvaruzkova, Z. Musilova, L. Palumbo, S. Sklenak and O. Gonsiorova, FTIR and ^{27}Al MAS NMR analysis of the effect of framework Al- and Si-defects in micro- and micro-mesoporous H-ZSM-5 on conversion of methanol to hydrocarbons, *Microporous Mesoporous Mater.*, 2011, **143**, 87–96.

22 D. Verboekend, A. M. Chabaneix, K. Thomas, J. P. Gilson and J. Pérez-Ramírez, Mesoporous ZSM-22 zeolite obtained by desilication: peculiarities associated with crystal morphology and aluminium distribution, *CrystEngComm*, 2011, **13**, 3408–3416.

23 J. Chen, Z. C. Feng, P. L. Ying and C. Li, ZnO clusters encapsulated inside micropores of zeolites studied by UV Raman and Laser-Induced luminescence spectroscopies, *J. Phys. Chem. B*, 2004, **108**, 12669–12676.

24 X. J. Niu, J. Gao, Q. Miao, M. Dong, G. F. Wang, W. B. Fan, Z. F. Qin and J. G. Wang, Influence of preparation method on the performance of Zn-containing HZSM-5 catalysts in methanol-to-aromatics, *Microporous Mesoporous Mater.*, 2014, **197**, 252–261.

25 Y. M. Liu, H. Q. Yang, F. Jin, Y. Zhang and Y. D. Li, Synthesis of pyridine and picolines over Co-modified HZSM-5 catalyst, *Chem. Eng. J.*, 2008, **136**, 282–287.

26 J. A. Biscardi, G. D. Meitzner and E. Iglesia, Structure and density of active Zn species in Zn/H-ZSM-5 propane aromatization catalysts, *J. Catal.*, 1998, **179**, 192–202.

27 H. Berndt, G. Lietz, B. Liicke and J. Volter, Zinc promoted H-ZSM-5 catalysts for conversion propane to aromatics I. Acidity and activity, *Appl. Catal., A*, 1996, **146**, 351–363.

28 H. Berndt, G. Lietz and J. Volter, Zinc promoted II. Nature of H-ZSM-5 catalysts for conversion of propane to aromatics the active sites and their activation, *Appl. Catal., A*, 1996, **146**, 365–379.